

Applying the BSS algorithm to the Chandra Deep Field South data

by F. Guglielmetti (MPE), H. Boehringer (MPE), R. Fischer (IPP), P. Rosati (ESO), P. Tozzi (INAF)

Abstract: A probabilistic two-component mixture model allows one to separate the diffuse background from the celestial sources within a one step algorithm without data censoring. The background is modelled with a thin-plate spline combined with the satellite's exposure time. Source probability maps (SPMs) are created in a multi-resolution analysis for revealing faint and extended sources. All detected sources are automatically parametrized to produce a list of source positions, fluxes and morphological parameters. The present analysis is applied to the *Chandra* Deep Field South (CDF-S) 2Ms public released data. Within its 1.884 ks of exposure time and its angular resolution (0.984 arcsec), the CDF-S data are particularly suited for testing the Background-Source separation (BSS) algorithm.

In *Figure 1*, the statistical detection of sources for one resolution and the background model are shown. In each panel right ascension versus declination is drawn. Note the well-defined background model, that provides reliable detections also at the field edge and on CCD gaps, where steep gradients in the data occurs.

An analysis is performed to test the internal consistency and the sensitivity of the BSS algorithm when detecting sources on real fields from pointed observations. Hence, a set of four images are extracted from the CDF-S 2Ms soft (0.5-2.0 keV) energy band. Each extracted image is characterized by the same fov of the CDF-S region and by 500ks exposure: these fields are indicated with numbers 1-4 CDF-S 500ks.

In *Figure 2*, the internal consistency of the BSS algorithm analyzing the four datasets is reported. The estimated positions (panels a-b) are consistent within each dataset with a precision of 1 arcsec. A larger scatter is found for the estimated fluxes and extents (panels c-d). The range of residuals extends to $\pm 3\sigma$. Poisson fluctuations in the background and contaminations by other sources in the field can increase the uncertainties estimated for the source flux and extent measurements. A sensitivity analysis is performed on the four CDF-S 500ks datasets and the results are compared to published ones: Giacconi et al. (2002) for the CDF-S 1Ms dataset; Luo et al. (2008) for the CDF-S 2Ms dataset.

In *Figure 3*, the logN-logS distribution is shown. The logN-logS distribution is computed from the sky

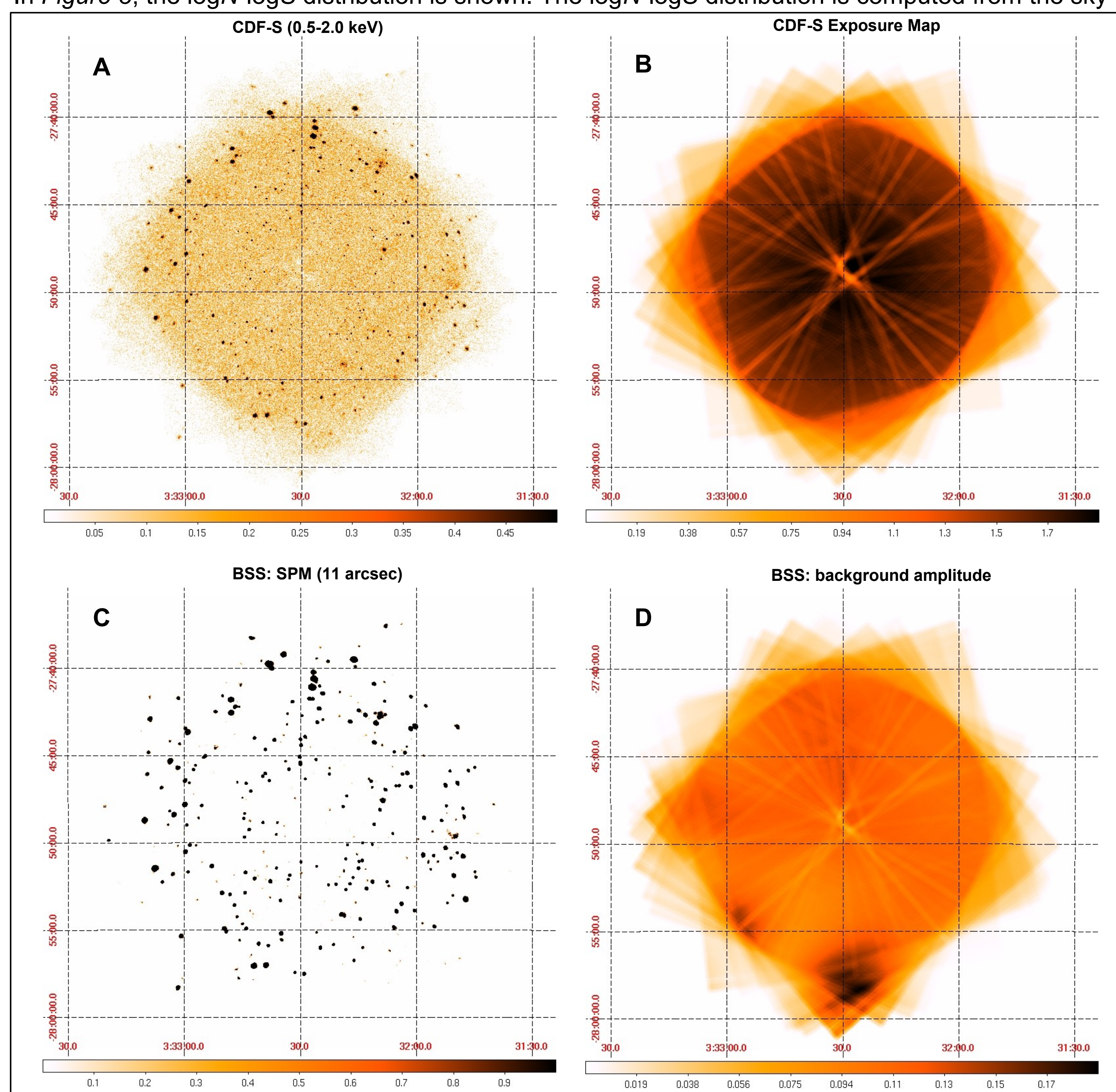


FIGURE 1: Example of joint estimation of background and sources with a two-component mixture model.

Panel A: CDF-S 2Ms photon count image in the soft (0.5-2.0 keV) energy band. The colorbar has units of count/pixel. The original scale of this image is in the range (0-959) count/pixel. The image is smoothed with a Gaussian kernel of 3 arcsec.

Panel B: Exposure map of the CDF-S 2Ms in the soft (0.5-2.0 keV) energy band. The colorbar has units of Ms/pixel.

Panel C: SPM at 11 arcsec resolution of the CDF-S 2Ms in the soft (0.5-2.0 keV) energy band as given by the BSS technique. The image is in linear scale. The colorbar indicates source probabilities per pixel. The image can be compared to panel A.

Panel D: Estimated background intensity of the CDF-S 2Ms in the soft (0.5-2.0 keV) energy band as given by the BSS technique. The image is in linear scale. The colorbar gives background count/pixel. The background map takes into account the variation in the exposure map, shown in panel B.

coverage. The sky coverage describes the sensitivity and the coverage of a survey. The logN-logS distribution provides information about the reliability of a survey. The sky coverage and the logN-logS distribution depends on the algorithm employed for source detection. The BSS background maps are used to construct the flux limit map in the sky coverage. Hence, vignetting effects and background variations are already accounted in the coverage.

The logN-logS distributions obtained with the four CDF-S 500ks datasets are in agreement with the published ones in Giacconi et al. (2002) and Luo et al. (2008).

Conclusions:

The BSS algorithm provides a robust technique. The BSS estimates in source parameters are internally consistent. No systematic errors are found within the BSS results. No contamination due to steep change in the exposure time map are shown in the background map and SPMs. The dynamic searching technique of the multiresolution analysis provides for the detection of a wide range of source fluxes.

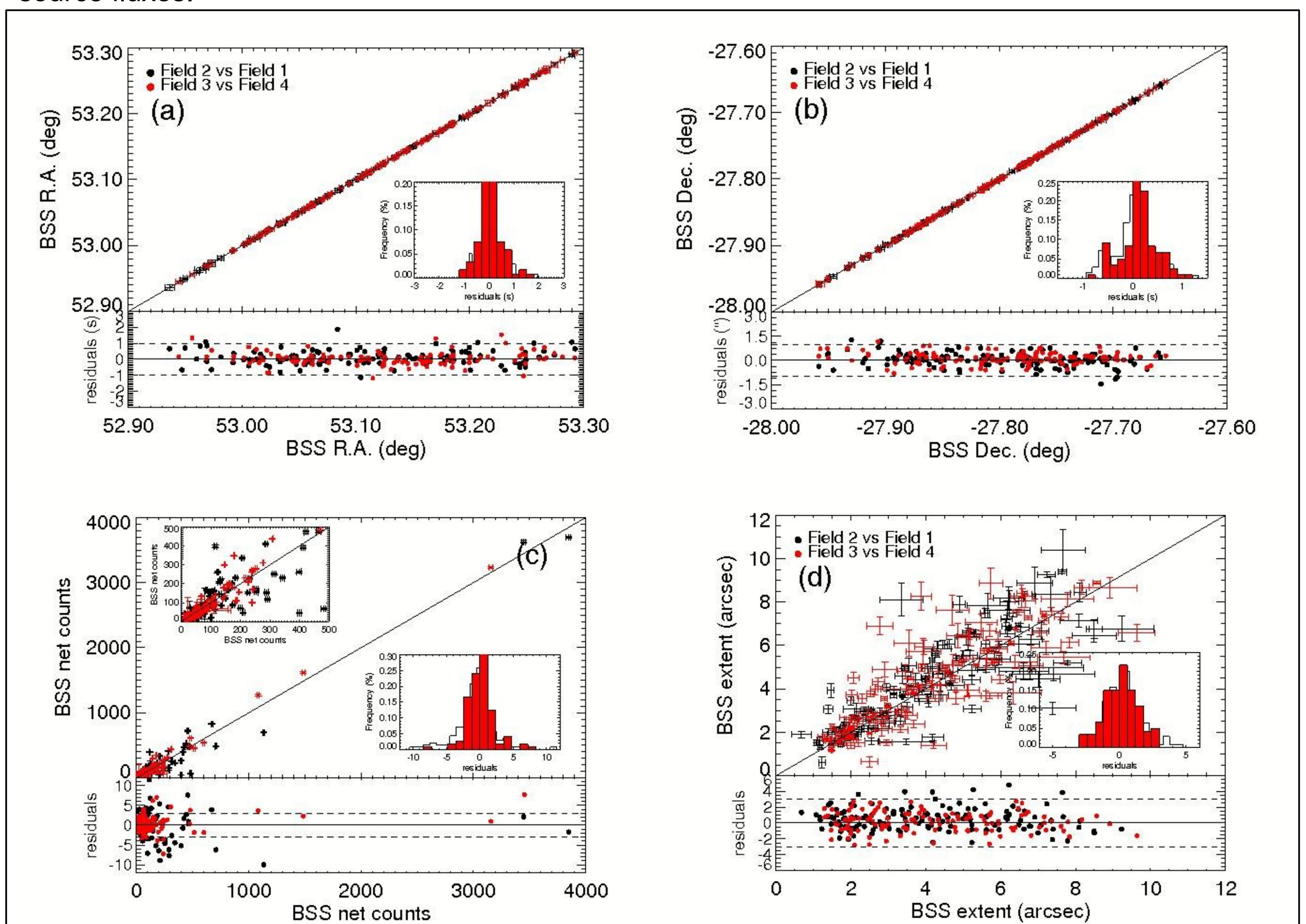


FIGURE 2: Comparison of the four CDF-S 500ks catalogs analyzed with the BSS algorithm.

The four CDF-S 500ks datasets are arranged in pairs. Fields 1 and 3 are compared to fields 2 and 4, respectively.

Panels (a-d): comparison of right ascension, declination, fluxes and size, respectively. 1σ errors are superposed.

In the upper plots, a line of equal values is drawn. The lower plots provide the residuals, i.e., the difference between the estimated values for each paired field. In panel (a-b) and (c-d) the residuals are the absolute difference and the relative error, respectively. The zero and the ± 1 arcsec lines (panels a-b) and the $\pm 3\sigma$ lines (panels c-d) are superposed with a continuous and dashed linestyles, respectively. Insets are added on the lower right-hand corner of each upper plot, i.e., the histogram plot of the residuals. The histograms show that the residuals are normally distributed. In addition, in Panel (c) a zoom into the data in the range value [0,500] net counts is shown in the upper left-hand corner.

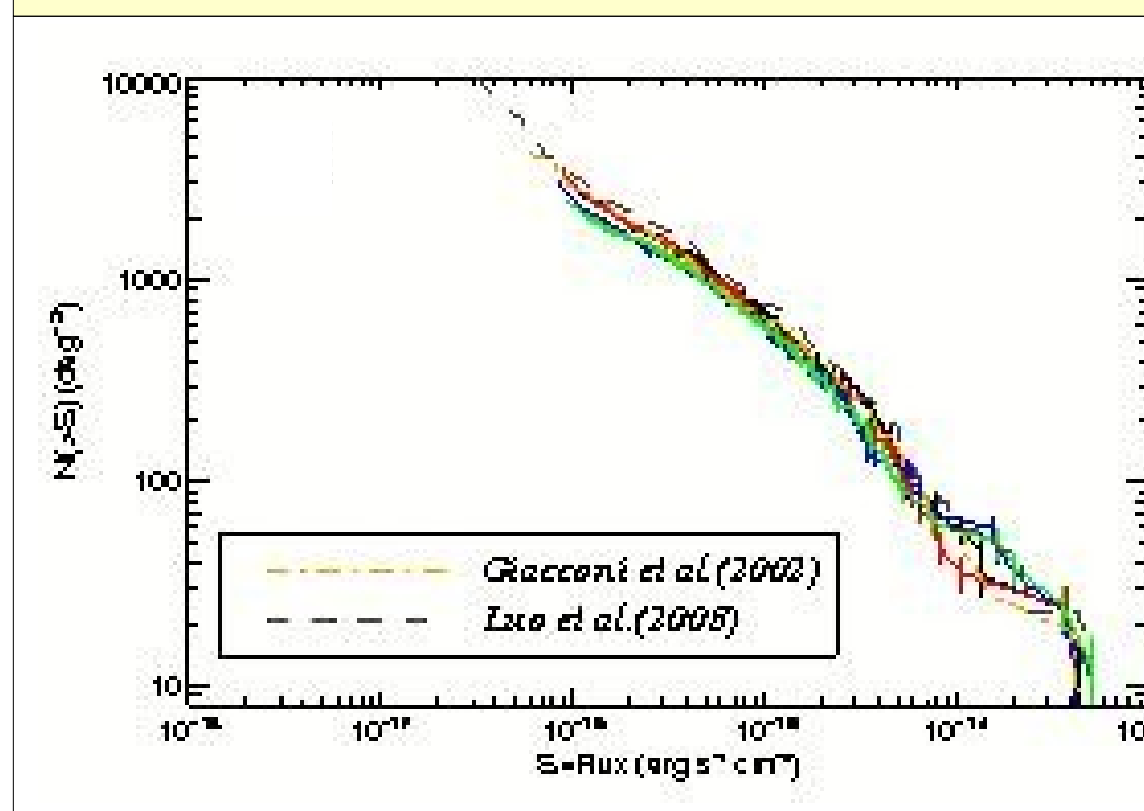


FIGURE 3: Sensitivity analysis of the BSS algorithm on the four CDF-S 500ks images.

The logN-logS distribution is created for each CDF-S 500ks image. Continuous lines in black, red, blue and green correspond to fields 1, 2, 3 and 4, respectively. The logN-logS distribution is obtained taking into account point-like sources, only. Each curve provides the number of sources per square degree of sky versus the minimum detectable flux.

References:

Guglielmetti F., Fischer R., Dose V., 2009, MNRAS, 396, 165
<http://edoc.ub.uni-muenchen.de/12732>